

Communication

# Differential Sensing of Antibiotics Using Metal Ions and Gold Nanoclusters Based on TMB–H<sub>2</sub>O<sub>2</sub> System

Suqin Liu <sup>1</sup>, Jinjie Wang <sup>1,2,\*</sup> , Yue Hu <sup>1</sup>, Yunjing Shi <sup>1</sup>, Jingxia Yang <sup>1</sup> and Min Zhang <sup>1,\*</sup>

<sup>1</sup> College of Chemistry and Chemical Engineering, Shanghai University of Engineering Science, 333 Longteng Road, Shanghai 201620, China; m040119510@sues.edu.cn (S.L.); m340121235@sues.edu.cn (Y.H.); m040118166@sues.edu.cn (Y.S.); jxyang@sues.edu.cn (J.Y.)

<sup>2</sup> Innovation Centre for Environment and Resources, Shanghai University of Engineering Science, 333 Longteng Road, Shanghai 201620, China

\* Correspondence: jinjiawang@sues.edu.cn (J.W.); zhangmin@sues.edu.cn (M.Z.); Tel.: +86-21-67791220 (M.Z.); +86-21-67791221 (J.W.)

**Abstract:** In the water system, antibiotic pollution significantly impacts the human body and the environment. Therefore, it is essential to quickly identify the types of antibiotics in the system and detect their concentration. It has been reported that many metal ions interact with antibiotics, and some of them can also change the enzyme-like catalytic properties of gold clusters (AuNCs). In the experiments, we found significant differences in the experimental results when different antibiotics and metal ions were placed in a TMB–H<sub>2</sub>O<sub>2</sub> system with AuNCs as catalysts. Based on this result, we devised a simple and sensitive colorimetric method for the simultaneous detection of multiple antibiotics using AuNCs–metal ions as the sensor, a multifunctional microplate detector as the detection instrument, and LDA as the analytical method. This method was successfully applied for the identification of antibiotics and the detection of their concentrations in river water.

**Keywords:** gold nanocluster; antibiotic; colorimetric detection; linear discriminant analysis; multiplex detection



**Citation:** Liu, S.; Wang, J.; Hu, Y.; Shi, Y.; Yang, J.; Zhang, M. Differential Sensing of Antibiotics Using Metal Ions and Gold Nanoclusters Based on TMB–H<sub>2</sub>O<sub>2</sub> System. *Chemosensors* **2022**, *10*, 222. <https://doi.org/10.3390/chemosensors10060222>

Academic Editor: Jun Wang

Received: 16 May 2022

Accepted: 9 June 2022

Published: 12 June 2022

**Publisher's Note:** MDPI stays neutral with regard to jurisdictional claims in published maps and institutional affiliations.



**Copyright:** © 2022 by the authors. Licensee MDPI, Basel, Switzerland. This article is an open access article distributed under the terms and conditions of the Creative Commons Attribution (CC BY) license (<https://creativecommons.org/licenses/by/4.0/>).

## 1. Introduction

Since the 20th century, the excessive use of antibiotics has led to residues of various antibiotics in water, food, and other environments. These antibiotics return to the human body through the action of biological circulation, causing harm to human health [1], such as loss of hearing, impairment of liver function, and kidney toxicity [2–5]. At the same time, the excessive residue of antibiotics also increases the resistance of bacteria, increasing the risk of disease transmission and difficulty of treatment [6,7]. Antibiotics can be divided into six categories according to their structure: aminoglycosides, quinolones, tetracyclines, polypeptides, β-lactams, and sulfonamides. At present, there are many methods for detecting antibiotics, such as microbiological methods [8], chromatography [9], spectral analysis [10], aptamer analysis [11], metal ion analysis [12], immunoassay [13], etc. Each of these methods has its advantages, but there are also some areas for improvement. For example, microbiological methods progress slowly [14]. High-performance liquid chromatography has high sensitivity and accuracy, but the pretreatment is complex and time-consuming [13]. Immunoassay and aptamer analysis have good sensitivity and specificity, but the prices of antibodies/aptamers are commonly high [15]. Therefore, it is essential to develop a rapid, low-cost, and straightforward method for detecting antibiotics. In detecting actual samples, it is necessary to detect multiple antibiotics simultaneously.

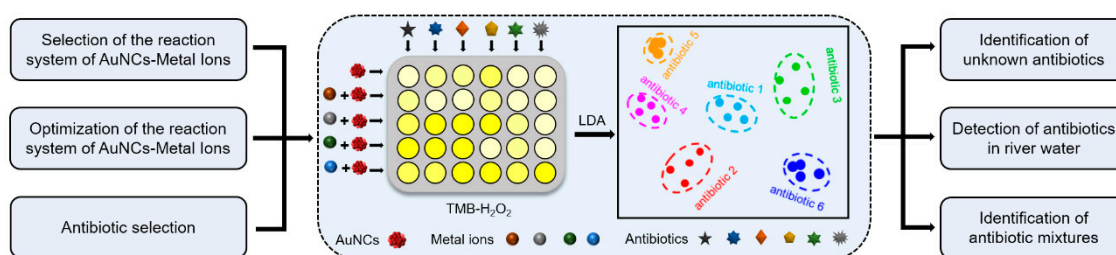
The metal ion method is an analysis method in which metal ions are used as the colorimetric reagent of the colorimetric sensor. A certain substance then reacts with the metal ions to cause color changes in the system [16–19]. Based on this principle, the complexation of antibiotics and metal ions allows for the detection of antibiotics. Chen et al.

designed a new method for detecting ciprofloxacin (Cip) by recovering the fluorescence intensity of the AuNCs-Cu<sup>2+</sup> system using Cip. The detection range is 0.4–50 ng mL<sup>-1</sup> and the detection limit is 0.3 ng mL<sup>-1</sup> [20]. Lu's group used the complexation of Cu<sup>2+</sup> with oxytetracycline (OTC), and Fe<sup>3+</sup> with norfloxacin (NOR) on micro-PAD analysis equipment ( $\mu$  PADS) successfully determined the OTC and NOR residues in pork [21]. All of these utilize the complexation between the metal ions and the antibiotics and have the characteristics of convenient operation and high sensitivity.

In addition, metal ions such as Fe<sup>3+</sup>, Cu<sup>2+</sup>, and Ag<sup>+</sup>, which interact with antibiotics, can affect the enzyme-like catalytic ability of gold nanoclusters (AuNCs) [22]. The catalytic performance of AuNCs can catalyze the decomposition of H<sub>2</sub>O<sub>2</sub>, and the generated reactive oxygen species (ROS) oxidize the peroxidase substrate 3,3',5,5'-tetramethylbenzidine (TMB) to blue ox1-TMB, which can be further oxidized to yellow ox2-TMB under the action of strong acid. Previous research by our group has shown that Cu<sup>2+</sup> could significantly enhance the catalytic activity of AuNCs, and we successfully used this system to detect glucose [23] and ppi [24]. Zhao's group constructed a detection method for Fe<sup>3+</sup> and Cu<sup>2+</sup> ions based on the effect of metal ions on the catalytic performance of glutathione-functionalized AuNCs [22]. Besides metal ions, the effect of antibiotics on the catalytic activity of AuNCs has also been reported: Song's research group found that tetracycline could increase the catalytic ability of AuNCs, thus constructing an analytical method to detect tetracycline [25]. Therefore, based on the effect of different metal ions on the catalytic performance of AuNCs and the degree of influence of different antibiotics on the system, we tried to construct a simple method that can detect multiple antibiotics simultaneously.

When testing multiple antibiotics simultaneously, distinguishing between antibiotics and the interference between various antibiotics are the main issues [26]. Linear discriminant analysis (LDA), widely used in pattern recognition, is a quantitative statistical approach for supervised dimensionality reduction and for classification [27,28]. It can classify multiple dependent variables through the relationship between independent and dependent variables and predict the dependent variables. Mao's team used the LDA method to distinguish between eight antibiotics tested simultaneously [29]. Yan's research group developed a new colorimetric sensor array and realized the identification of a variety of bacteria through LDA, which has potential in the field of diagnosis of clinical urine and serum samples [30].

Herein, we report a method for the simultaneous detection of multiple antibiotics using AuNCs-metal ions as the sensor, a multifunctional microplate reader as the detection instrument, and LDA as the analytical method. Six antibiotics (TC, CTC, OTC, Cip, Van, and GM), belonging to tetracycline, quinolone, aminoglycoside, and polypeptide categories, were selected as the target analytes in this study. The experimental process was as follows (Scheme 1). Firstly, the metal ions that affected the AuNCs catalysis and the antibiotics that had complexation with metal ions were screened out. Secondly, the feasibility of the AuNCs-metal ions system for the detection of specific antibiotics was confirmed. Thirdly, the detection conditions of different systems were studied. Fourthly, LDA was used as an analytical tool to construct a method for detecting multiple antibiotics. Finally, the practical application prospect of this method was proved by the detection results of unknown antibiotics.



**Scheme 1.** The schematic diagram of recognition and detection of antibiotics by metal ions and AuNCs based on TMB-H<sub>2</sub>O<sub>2</sub> system.

## 2. Materials and Methods

### 2.1. Materials

Gold chloride trihydrate ( $\text{HAuCl}_4 \cdot 3\text{H}_2\text{O}$ , 99.9%), 3,3',5,5'-tetramethylbenzidine (TMB), and gentamycin sulfate (GM) were supplied by Aladdin Chemistry Co. Ltd. (Shanghai, China). Tetracycline hydrochloride (TC), chlortetracycline hydrochloride (CTC), oxytetracycline (OTC), ciprofloxacin hydrochloride (Cip), and vancomycin hydrochloride (Van) were purchased from Sangon Biotech Co. Ltd. (Shanghai, China).  $\text{H}_2\text{O}_2$ ,  $\text{Cu}(\text{NO}_3)_2$ ,  $\text{AgNO}_3$ ,  $\text{FeCl}_3$ ,  $\text{FeSO}_4 \cdot 4\text{H}_2\text{O}$ ,  $\text{Al}_2(\text{SO}_4)_3 \cdot 18\text{H}_2\text{O}$ ,  $\text{Zn}(\text{NO}_3)_2$ ,  $\text{Ce}(\text{NO}_3)_3$ ,  $\text{Pb}(\text{NO}_3)_2$ ,  $\text{CdSO}_4 \cdot 8\text{H}_2\text{O}$ ,  $\text{CrCl}_3 \cdot 6\text{H}_2\text{O}$ , and  $\text{Ni}(\text{NO}_3)_2$  were obtained from Sinopharm Chemical Reagent Co. Ltd. (Shanghai, China).

Britton–Robinson (BR) buffer (pH = 3.0–5.0) was prepared with 0.04 M phosphoric acid, acetic acid, and boric acid, and the pH value was adjusted with 0.2 M NaOH.

### 2.2. Preparation of AuNCs

AuNCs were synthesized by the method reported in the literature [23] using Keratin as a template. According to the research group's previous research on AuNCs, the particle size of AuNCs is about 2 nm. The prepared AuNCs were purified by size exclusion chromatography (Sephadex G25) and stored at 4 °C.

### 2.3. Selection and Optimization of the Reaction System of AuNCs-Metal Ions

TMB- $\text{H}_2\text{O}_2$  is a common enzyme-like catalytic system. When a catalyst with enzyme-like catalytic properties exists in the system, the catalyst can catalyze the decomposition of  $\text{H}_2\text{O}_2$  into ROS. ROS can oxidize colorless TMB to blue ox1-TMB, thus changing the absorption of the solution. The blue ox1-TMB is further oxidized to yellow ox2-TMB under the action of strong acid.

The selection of the AuNCs-metal ions reaction system was based on the effect of different ions on the catalytic efficiency of AuNCs. When metal ions were added to the AuNCs- $\text{H}_2\text{O}_2$ -TMB reaction system, a large change in the absorbance of the reaction solution was desirable. The experimental procedure was as follows. First, 78  $\mu\text{L}$  AuNCs ( $5.79 \text{ mg mL}^{-1}$ ), 10  $\mu\text{L}$  different metal ions ( $\text{Ag}^+$ ,  $\text{Fe}^{3+}$ ,  $\text{Fe}^{2+}$ ,  $\text{Al}^{3+}$ ,  $\text{Zn}^{2+}$ ,  $\text{Ce}^{3+}$ ,  $\text{Pb}^{2+}$ ,  $\text{Cd}^{2+}$ ,  $\text{Cr}^{3+}$ ,  $\text{Ni}^{2+}$ ; 900  $\mu\text{M}$ ), and 773  $\mu\text{L}$  BR buffer (pH = 4) were left at room temperature for 5 min, and then 30  $\mu\text{L}$   $\text{H}_2\text{O}_2$  (3 mM or 300 mM) and 9  $\mu\text{L}$  TMB ( $10 \text{ mg mL}^{-1}$ ) were added and reacted at 40 °C for 30 min. Then, the reaction solution was centrifuged at 12,000 rpm for 2 min, and the precipitate was reconstituted with half of the original reaction volume of  $\text{H}_2\text{SO}_4$  (2 M) solution and centrifuged again. The absorbance of the supernatant (452 nm) was measured by a multifunctional microplate reader (INFINITE 200 PRO, Mannedorf, Switzerland).

At the same time, the concentration of  $\text{H}_2\text{O}_2$  (100–400  $\mu\text{M}$  or 10–40 mM) and the BR buffer solution (pH = 3.0–5.0) of the selected AuNCs-metal ions system were optimized.

Furthermore, as a critical detection instrument in this study, the multifunctional microplate reader has the characteristics of more convenient and faster detection compared with a traditional UV-visible spectrophotometer. The multifunctional microplate reader's sensitivity, accuracy, and stability were tested. The results showed that the experimental data detected by the microplate reader were very stable, and the absorbance intensity detected by the microplate was about 0.4 times as much as the data detected by the spectrophotometer (Table S1 and Figure S1). Specific test parameters and experimental results are in the supporting information.

### 2.4. Detection of Antibiotics Based on AuNCs-Metal Ions Reaction System

According to the selected AuNCs-metal ions reaction system (AuNCs- $\text{Cu}^{2+}$ , AuNCs- $\text{Fe}^{3+}$ , AuNCs- $\text{Fe}^{2+}$ , and AuNCs- $\text{Ag}^+$ ), six antibiotics (TC, CTC, OTC, Cip, Van, and GM) were selected as the target analytes in this study. Antibiotics detection was as follows: ten  $\mu\text{L}$  of metal ions ( $\text{Cu}^{2+}$ ,  $\text{Fe}^{3+}$ ,  $\text{Fe}^{2+}$ : 450  $\mu\text{M}$ ;  $\text{Ag}^+$ , 900  $\mu\text{M}$ ) and 450  $\mu\text{L}$  of different concentrations of antibiotics were incubated with 323  $\mu\text{L}$  of BR buffer (pH = 4 or 4.5) at

room temperature for 5 min, and then the mixture was incubated with 78  $\mu\text{L}$  of AuNCs ( $5.79 \text{ mg mL}^{-1}$ ) at room temperature for 5 min. Then, 30  $\mu\text{L}$  of  $\text{H}_2\text{O}_2$  (9 mM or 600 mM) and 9  $\mu\text{L}$  of TMB ( $10 \text{ mg mL}^{-1}$ ) were added and reacted at  $40^\circ\text{C}$  for 30 min. Then, the reaction solution was centrifuged, redissolved with  $\text{H}_2\text{SO}_4$  (2 M) solution, and centrifuged again, and finally, the absorbance of the supernatant at 452 nm was detected by a multifunctional microplate reader.

The application of this sensing platform for multicomponent antibiotics was also investigated. The 11 antibiotic mixtures included 8 mixtures of two antibiotics, 2 mixtures of three antibiotics, and 1 mixture that included six antibiotics. The amount of antibiotics in the mixture was in equal proportion. For example, TC + CTC = 50% TC + 50% CTC, TC + OTC + CTC = 33.3% TC + 33.3% OTC + 33.3% CTC. The procedure was the same as that for single component antibiotic detection.

### 2.5. Antibiotics Identification

The LDA method was used for the identification of antibiotics. The values of  $I/I_0$  were analyzed by LDA, where  $I$  is the absorbance value of the AuNCs-metal ions reaction system after adding antibiotics, and  $I_0$  is the absorbance value of the system without antibiotics. With the six systems as independent variables and the type of antibiotic as a dependent variable, the processed data were imported into SPSS Statistics 17.0 software for LDA analysis.

## 3. Results and Discussion

### 3.1. Effects of Metal Ions on the Catalytic Performance of AuNCs

This study attempted to construct a multicomponent antibiotic detection method based on the interaction between metal ions, antibiotics, and AuNCs. Firstly, we used the TMB- $\text{H}_2\text{O}_2$  system to screen out the metal ions that affect the catalysis of AuNCs. In the current study of the TMB- $\text{H}_2\text{O}_2$  system, the range of  $\text{H}_2\text{O}_2$  concentrations is wide (100  $\mu\text{M}$ –50 mM), and the corresponding experimental results are quite different [31–33].

Therefore, we selected TMB- $\text{H}_2\text{O}_2$  systems with two  $\text{H}_2\text{O}_2$  concentrations of 100  $\mu\text{M}$  and 10 mM (L- $\text{H}_2\text{O}_2$  and H- $\text{H}_2\text{O}_2$ ) to screen some common metal ions ( $\text{Cu}^{2+}$ ,  $\text{Fe}^{3+}$ ,  $\text{Fe}^{2+}$ ,  $\text{Ag}^+$ ,  $\text{Al}^{3+}$ ,  $\text{Zn}^{2+}$ ,  $\text{Ce}^{3+}$ ,  $\text{Pb}^{2+}$ ,  $\text{Cd}^{2+}$ ,  $\text{Cr}^{3+}$ , and  $\text{Ni}^{2+}$ ) in this experiment (Figure 1). As shown in Figure 1a, when the concentration of  $\text{H}_2\text{O}_2$  is 100  $\mu\text{M}$ , the absorbance of the reaction system containing  $\text{Cu}^{2+}$ ,  $\text{Fe}^{3+}$ , and  $\text{Fe}^{2+}$  ions was greatly improved compared with the blank sample without metal ions, indicating that the presence of these three metal ions significantly improves the catalytic performance of AuNCs. The presence of  $\text{Ag}^+$  ions also resulted in a slight improvement in the catalytic performance of AuNCs. When the concentration of  $\text{H}_2\text{O}_2$  was 10 mM, the experimental results were quite different (Figure 1b). The presence of  $\text{Ag}^+$  ions obviously inhibited the catalytic performance of AuNCs. The absorbance of the reaction system containing  $\text{Fe}^{3+}$  and  $\text{Cd}^{2+}$  ions also decreased slightly. According to the detection results of the TMB- $\text{H}_2\text{O}_2$  system under two different concentrations of  $\text{H}_2\text{O}_2$ , we chose AuNCs- $\text{Cu}^{2+}$ , AuNCs- $\text{Fe}^{3+}$ , AuNCs- $\text{Fe}^{2+}$  (L- $\text{H}_2\text{O}_2$ ), and AuNCs- $\text{Ag}^+$  (H- $\text{H}_2\text{O}_2$ ) as the reaction system for the subsequent detection of antibiotics.

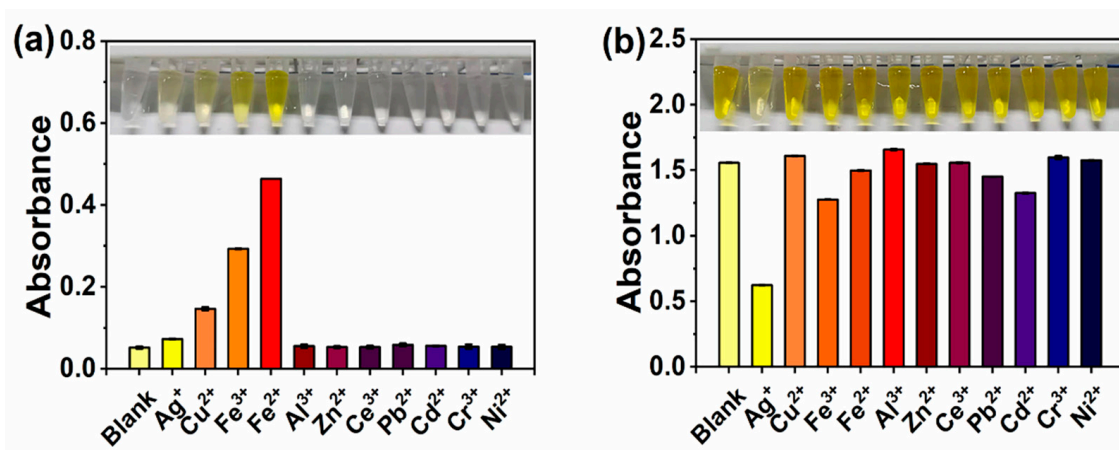


**Figure 1.** Effects of metal ions on the catalytic activity of AuNCs using the TMB–H<sub>2</sub>O<sub>2</sub> system with two H<sub>2</sub>O<sub>2</sub> concentrations of 100 μM (a) and 10 mM (b). Insets are photos of samples of different reaction systems under visible light.

### 3.2. Optimization of the Reaction System of AuNCs-Metal Ions

In the four selected reaction systems, the H<sub>2</sub>O<sub>2</sub> concentration and pH value were optimized, respectively, to improve the sensitivity of the detection method. The optimization principle was to select conditions with greater variation compared to the control AuNCs system. The detection results of AuNCs-Cu<sup>2+</sup>, AuNCs-Fe<sup>3+</sup> and AuNCs-Fe<sup>2+</sup> reaction systems with low H<sub>2</sub>O<sub>2</sub> concentration are shown in Figure S2. The detection results of AuNCs-Ag<sup>+</sup> with high H<sub>2</sub>O<sub>2</sub> concentration are shown in Figure S3. The detection conditions of each reaction system were as follows: AuNCs-Cu<sup>2+</sup> (C<sub>H<sub>2</sub>O<sub>2</sub></sub> = 300 μM, pH = 4.5), AuNCs-Fe<sup>3+</sup> (C<sub>H<sub>2</sub>O<sub>2</sub></sub> = 300 μM, pH = 4), AuNCs-Fe<sup>3+</sup> (C<sub>H<sub>2</sub>O<sub>2</sub></sub> = 300 μM, pH = 4), and AuNCs-Ag<sup>+</sup> (C<sub>H<sub>2</sub>O<sub>2</sub></sub> = 20 mM, pH = 4.5).

### 3.3. The Feasibility and Proposed Mechanism of Detecting Antibiotics with AuNCs-Metal Ions Reaction System

For four AuNCs-metal ions reaction systems, six antibiotics (TC, OTC, CTC, Cip, Van, and GM) were selected as detection targets based on the literature review [3,34–41] of the interaction between metal ions and antibiotics (Table S2). Six antibiotics were added to four AuNCs-metal ions reaction systems and two control AuNCs reaction systems to verify the feasibility of this method (Figure 2).  $I$  is the absorbance value of the reaction solution in the presence of the antibiotic and  $I_0$  is the absorbance value of the same system without the antibiotic.  $I/I_0 > 1$  indicates that the addition of the antibiotic increased the absorbance of the reaction system.  $I/I_0 < 1$  represents that the addition of the antibiotic reduced the absorbance of the reaction system. The results in Figure 2b indicate that most of the antibiotics affected the absorbance of the AuNCs-metal ions reaction system.

However, the effects of some antibiotics on the AuNCs-metal ions system were different from our expectations. We expected that antibiotics would complex with metal ions and then weaken the effect of metal ions on the catalytic ability of AuNCs. The only antibiotics that met our expectations were Van and GM. According to the literature [36,38], Fe<sup>3+</sup> and Ag<sup>+</sup> combine with amino nitrogen atoms and carbonyl oxygen atoms in antibiotic molecules to form stable complexes (Fe<sup>3+</sup>-Van, Ag<sup>+</sup>-GM), which can reduce the concentration of Fe<sup>3+</sup> and Ag<sup>+</sup> in the solution, leading to the weakening of the influence of metal ions on the catalytic activity of AuNCs. In addition, the catalytic performance of AuNCs decreased when Van was present in the AuNCs-Fe<sup>2+</sup> reaction system, which may be due to the presence of Fe<sup>3+</sup> ions in the AuNCs-Fe<sup>2+</sup> reaction system due to the Fenton reaction.

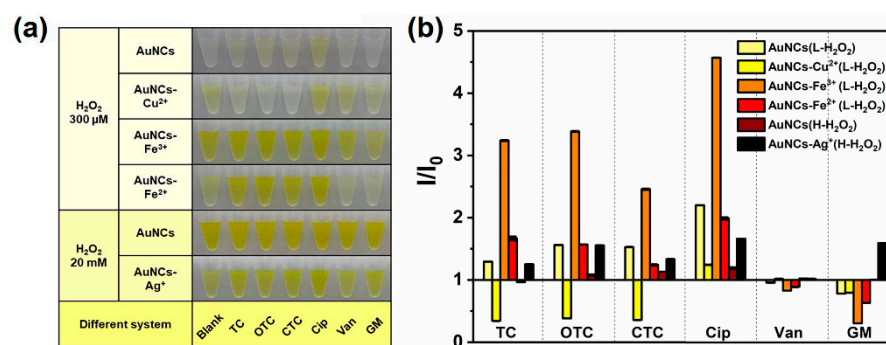


**Figure 2.** (a) Color changes of 6 antibiotics in different AuNCs-metal ions reaction systems under visible light. (b) The absorbance response at 452 nm ( $I/I_0$ ) of sensor array against various antibiotics. Reaction conditions: AuNCs, 0.5 mg mL<sup>-1</sup>; Cu<sup>2+</sup>, Fe<sup>3+</sup>, Fe<sup>2+</sup>, 5 μM; Ag<sup>+</sup>, 10 μM; antibiotics, 15 μM; H<sub>2</sub>O<sub>2</sub>, 300 μM (L-H<sub>2</sub>O<sub>2</sub>); TMB, 0.1 mg mL<sup>-1</sup> and 20 mM (H-H<sub>2</sub>O<sub>2</sub>).

To verify the interaction mechanism of the other four antibiotics with AuNCs and metal ions, the fluorescence intensity of each system was also characterized (Figure 3). In Figure 3, each system contains 0.25 mg mL<sup>-1</sup> AuNCs, 10 μM metal ions and 15 μM target antibiotics. According to the variety of absorbance value and fluorescence intensity of each reaction system and the records of related literature, we believe that antibiotics not only interacted with metal ions but also interacted with AuNCs, and there were not only competitive but also synergistic relationships among them. The proposed mechanism is shown in Scheme 2.

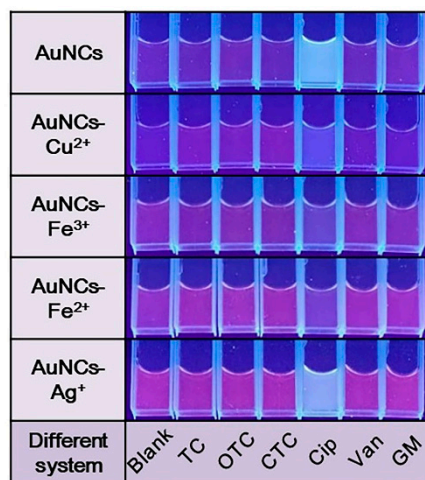
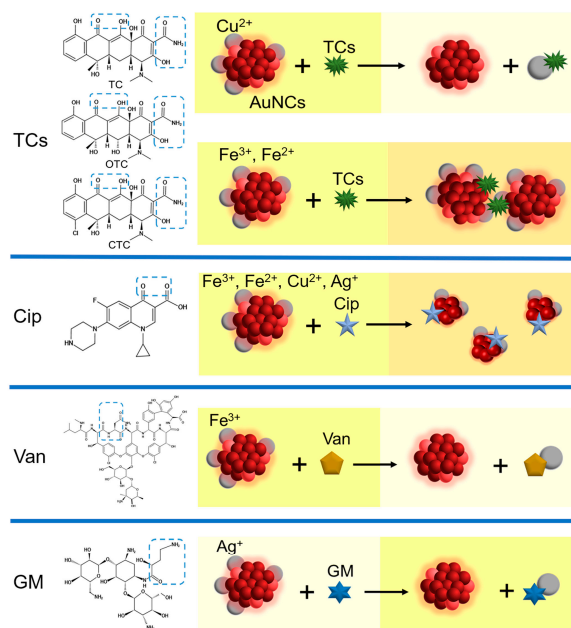


**Figure 3.** Photographs of the color change of 6 antibiotics in different AuNCs-metal ions systems under UV light (302 nm). Reaction conditions: AuNCs, 0.25 mg mL<sup>-1</sup>; metal ions, 10 μM; antibiotics, 15 μM.

TC, OTC, and CTC were all tetracyclines (TCs) with similar structures and had the same effect on the reaction systems. The absorbance of the AuNCs (L-H<sub>2</sub>O<sub>2</sub>) system increased when tetracyclines were present in the system, indicating that tetracycline could enhance the catalytic performance of AuNCs. Liu et al. showed by Zate potential that there was a strong electrostatic interaction between tetracyclines and AuNCs, resulting in electron transfer between the two, which increased the amount of Au<sup>3+</sup> on the surface of AuNCs and enhanced the catalytic activity of AuNCs [25,42]. In Figure 2, the catalytic performance of AuNCs was increased when tetracyclines existed in the AuNCs-Fe<sup>3+</sup>, AuNCs-Fe<sup>2+</sup>, and AuNCs-Ag<sup>+</sup> reaction systems, indicating the interaction between tetracyclines and AuNCs was more significant than that between tetracyclines and Fe<sup>2+</sup>, Fe<sup>3+</sup>, and Ag<sup>+</sup> ions. The AuNCs-Cu<sup>2+</sup> reaction system was an exception, because tetracyclines have a

higher complexation constant with  $\text{Cu}^{2+}$  ions [35], resulting in a decrease in the catalytic performance of AuNCs.



**Scheme 2.** The schematic diagram of the interaction mechanism of antibiotics with AuNCs and metal ions in TMB- $\text{H}_2\text{O}_2$  system.

The interaction between Cip and AuNCs was unique. Cip can decompose AuNCs to generate ROS and promote the oxidation of TMB [43]. As shown in Figure 3, the addition of Cip resulted in a large blue shift in the fluorescence emission peak of AuNCs, indicating that the size of AuNCs was getting smaller. In the presence of  $\text{Cu}^{2+}$ ,  $\text{Fe}^{2+}$ , and  $\text{Fe}^{3+}$  ions, metal ions could react with the keto and the carboxylic acid oxygen in Cip ligand to form the corresponding complexes, which could weaken this phenomenon [34,39]. However, in general, the influence of Cip on the catalysis of AuNCs was more significant than that of other metal ions.

### 3.4. Detection of Antibiotics with AuNCs-Metal Ions Reaction System

In Figure 2, the sensor array, which is composed of a AuNCs-metal ions reaction system, shows unique absorbance recognition patterns for six selected antibiotics. The LDA method was used to analyze the relevant data to study the pattern recognition ability of the sensor array for various antibiotics. The absorbance values of each reaction system were analyzed by LDA, which transformed the training matrix (6 systems  $\times$  6 antibiotics  $\times$  5 concentrations) into canonical scores and had a visual two-dimensional (2D) plot under the 95% confidence ellipses. The six systems were AuNCs, AuNCs- $\text{Cu}^{2+}$ , AuNCs- $\text{Fe}^{3+}$  and AuNCs- $\text{Fe}^{2+}$  ( $\text{L-H}_2\text{O}_2$ ) and AuNCs, and AuNCs- $\text{Ag}^+$  ( $\text{H-H}_2\text{O}_2$ ) reaction systems. The six antibiotics were TC, OTC, CTC, Cip, Van, and GM. The five concentrations of antibiotics were 50, 250, 500, 2500, and 5000 nM. The detailed data are in Table S3. The data matrix was imported into the SPSS Statistics 17.0 data processor for LDA discriminant analysis. The analysis shows that the data matrix is analyzed using five typical discriminant functions and transformed into five functional factors. They accounted for 68.4%, 23.6%, 6.4%, 1.2%, and 0.4%, respectively. Each factor represents its contribution to the overall classification. The combined contribution of factor 1 and factor 2 was 92%, so factor 1 and factor 2 could be used to construct a visual two-dimensional (2D) map (Figure 4a). In Figure 4a, all target antibiotics were separated without any overlap. The two-dimensional (2D) plot for colorimetric response patterns demonstrated the excellent ability of this sensor array in multiple antibiotics discrimination.

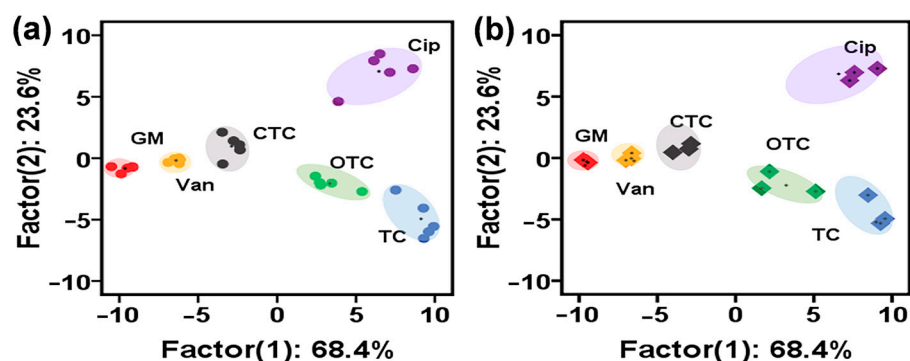


**Figure 4.** (a) LDA plot for the discrimination result with 95% confidence ellipses. Each point represents the response pattern for a single antibiotics sample against AuNCs-metal ions reaction systems. (b) Identification results of unknown antibiotics in river water.

After identifying the antibiotics, it was also important to quantitatively detect them. Therefore, we used a multifunctional microplate reader to detect the absorbance values of different concentrations of antibiotics in each system, and the results are shown in Figures S4–S9. There were six sets of absorbance–concentration data for each antibiotic in different reaction systems. For the convenience and accuracy of data processing, the data of two reaction systems related to each antibiotic were selected to draw and fit the standard curves. The selection criterion was to choose the two most sensitive systems. If there were different response trends (positive and negative), then we selected the sensitive system in each of the two response trends. The associated fitting formulas are listed in Table S4, where Y is the absorbance of the sample solution at 452 nm, and X is the concentration of antibiotics. The detection range of each antibiotic was from 5 to 15,000 nM.

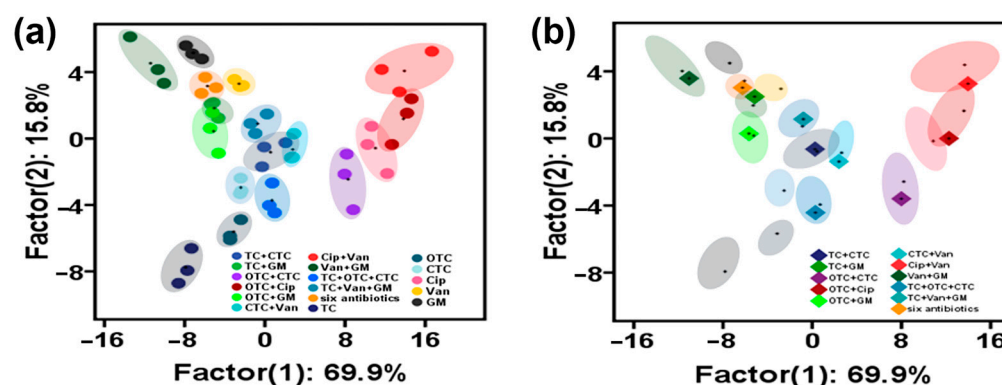
To verify the feasibility of the AuNCs-metal ions system for the analysis of unknown antibiotics, the recognition and determination of antibiotic levels in river water were performed. River water was collected from Zhangjiabang River on the campus of the Shanghai University of Engineering Science. The river water was treated at 12,000 rpm for 5 min and further filtered with a 0.22  $\mu\text{m}$  membrane [44]. Then, various antibiotics with different concentrations (80, 800, and 8000 nM) were mixed into the river water for detection and analysis. Figure 4b shows that all the samples were correctly identified with 100% accuracy for the six unknown antibiotics with different concentrations. Specific data and identification results are shown in Table S5. At the same time, the concentration of antibiotic samples was detected based on the obtained standard curve. The recovery data in Table 1 were the average calculated results of two selected standard curves (Table S6). In Table 1, the recoveries of 18 unknown samples ranged from 93.39% to 108.67%, indicating that the colorimetric method based on the AuNCs-metal ions system had great potential for detecting antibiotics in river water.

### 3.5. Classification and Identification of Multicomponent Antibiotics

In addition, we further evaluated the potential ability of this AuNCs-metal ions sensor array to discriminate complex antibiotic mixtures. As shown in Figure 5a, the colorimetric response patterns for 11 antibiotic mixtures and 6 pure antibiotics were clearly distinguished in the LDA plot. The original data are shown in Table S7. As shown in Figure 5b, mixed antibiotics (800 nM) were added to the river water for detection. The results showed that the method performed well in the simultaneous identification of 11 antibiotic mixtures, and the classification accuracy was 100%. The specific data and identification results are shown in Table S8.

**Table 1.** Recovery results for antibiotic detection in river water. See Table S6 for detailed data.

Antibiotics	Original (nM)	Spiked (nM)	Found (nM)	Recovery (%)
TC	not detected	80	82.85	103.56
	not detected	800	868.04	108.51
	not detected	8000	7695.51	96.19
OTC	not detected	80	76.80	96.00
	not detected	800	748.15	93.52
	not detected	8000	7907.34	98.84
CTC	not detected	80	84.58	105.72
	not detected	800	859.27	107.41
	not detected	8000	8088.48	101.12
Cip	not detected	80	82.18	102.72
	not detected	800	834.51	104.31
	not detected	8000	8693.04	108.67
Van	not detected	80	85.33	106.66
	not detected	800	847.50	105.94
	not detected	8000	7892.36	98.65
GM	not detected	80	85.56	106.93
	not detected	800	747.14	93.39
	not detected	8000	7787.14	97.34

**Figure 5.** (a) LDA plot for the discrimination result of antibiotics mixtures with 95% confidence ellipses. (b) Identification results of unknown mixed antibiotics in river water.

#### 4. Conclusions

In this research, a colorimetric sensor array for antibiotic detection was successfully developed based on the interaction between AuNCs, metal ions, and antibiotics in a TMB-H<sub>2</sub>O<sub>2</sub> reaction system. The accurate identification of unknown antibiotics can be achieved by analyzing the absorbance values of the sensing array through the LDA method. Then, the concentration of the identified antibiotic can be accurately detected by matching with its standard curve. Furthermore, the sensor array can be used to determine antibiotic mixtures in river water. The colorimetric strategy of combining AuNCs, antibiotics, and other ions that interact with them is expected to be applied to identifying and detecting antibiotics in water.

**Supplementary Materials:** The following supporting information can be downloaded at: <https://www.mdpi.com/article/10.3390/chemosensors10060222/s1>. Figure S1: Comparison of multifunctional microplate reader and UV-Vis spectrophotometer; Table S1: Comparison of detection modes of a multifunctional microplate reader; Figure S2: Optimization of the reaction conditions of the reaction system (L-H<sub>2</sub>O<sub>2</sub>); Figure S3: Optimization of reaction conditions of the reaction system (H-H<sub>2</sub>O<sub>2</sub>); Table S2: Summary of the interaction between the antibiotic and metal ions reported in the literature; Table S3: LDA identification results of 6 antibiotics with different concentrations; Figure S4: The

dose-response curves for TC detection using (a) AuNCs, (b) AuNCs-Cu<sup>2+</sup>, (c) AuNCs-Fe<sup>3+</sup>, (d) AuNCs-Fe<sup>2+</sup>, (e) AuNCs, (f) AuNCs-Ag<sup>+</sup> reaction system, between the absorbance at 452 nm against the logarithmic concentration of TC; Figure S5: The dose-response curves for OTC detection using (a) AuNCs, (b) AuNCs-Cu<sup>2+</sup>, (c) AuNCs-Fe<sup>3+</sup>, (d) AuNCs-Fe<sup>2+</sup>, (e) AuNCs, (f) AuNCs-Ag<sup>+</sup> reaction system, between the absorbance at 452 nm against the logarithmic concentration of OTC; Figure S6: The dose-response curves for CTC detection using (a) AuNCs, (b) AuNCs-Cu<sup>2+</sup>, (c) AuNCs-Fe<sup>3+</sup>, (d) AuNCs-Fe<sup>2+</sup>, (e) AuNCs, (f) AuNCs-Ag<sup>+</sup> reaction system, between the absorbance at 452 nm against the logarithmic concentration of CTC; Figure S7: The dose-response curves for Cip detection using (a) AuNCs, (b) AuNCs-Cu<sup>2+</sup>, (c) AuNCs-Fe<sup>3+</sup>, (d) AuNCs-Fe<sup>2+</sup>, (e) AuNCs, (f) AuNCs-Ag<sup>+</sup> reaction system, between the absorbance at 452 nm against the logarithmic concentration of Cip; Figure S8: The dose-response curves for Van detection using (a) AuNCs, (b) AuNCs-Cu<sup>2+</sup>, (c) AuNCs-Fe<sup>3+</sup>, (d) AuNCs-Fe<sup>2+</sup>, (e) AuNCs, (f) AuNCs-Ag<sup>+</sup> reaction system, between the absorbance at 452 nm against the logarithmic concentration of Van; Figure S9: The dose-response curves for GM detection using (a) AuNCs, (b) AuNCs-Cu<sup>2+</sup>, (c) AuNCs-Fe<sup>3+</sup>, (d) AuNCs-Fe<sup>2+</sup>, (e) AuNCs, (f) AuNCs-Ag<sup>+</sup> reaction system, between the absorbance at 452 nm against the logarithmic concentration of GM; Table S4: Summary of the fitting curve formula in Figures S4–S9; Table S5: Identification of unknown 18 antibiotics samples in river water; Table S6: Recovery results for antibiotics detection in river water samples using AuNCs-metal ions system; Table S7: LDA identification results of 11 mixture antibiotics and 6 antibiotics with different concentrations; Table S8: Identification of unknown 11 mixture antibiotics samples in river water.

**Author Contributions:** Conceptualization, J.W.; Investigation, S.L. and Y.S.; Methodology, J.W.; Resources, Y.H.; Supervision, J.W.; Validation, S.L.; Writing—original draft, S.L.; Writing—review & editing, J.Y. and M.Z. All authors have read and agreed to the published version of the manuscript.

**Funding:** This research was funded by NSFC (Grants 21806103) and the Capacity Building Project of Some Local Colleges and Universities in Shanghai (No. 21010501400).

**Institutional Review Board Statement:** Not applicable.

**Informed Consent Statement:** Not applicable.

**Data Availability Statement:** Not applicable.

**Conflicts of Interest:** The authors declare no conflict of interest.

## References

1. Wu, D.L.; Zhang, M.; He, L.X.; Zou, H.Y.; Liu, Y.S.; Li, B.B.; Yang, Y.Y.; Liu, C.; He, L.Y.; Ying, G.G. Contamination profile of antibiotic resistance genes in ground water in comparison with surface water. *Sci. Total Environ.* **2020**, *715*, 136975. [[CrossRef](#)] [[PubMed](#)]
2. Mohammadzadeh, M.; Montaseri, M.; Hosseinzadeh, S.; Majlesi, M.; Berizi, E.; Zare, M.; Derakhshan, Z.; Ferrante, M.; Conti, G.O. Antibiotic residues in poultry tissues in iran: A systematic review and meta-analysis. *Environ. Res.* **2021**, *204*, 112038. [[CrossRef](#)] [[PubMed](#)]
3. Liu, Z.; Hou, J.; Wang, X.; Hou, C.; Ji, Z.; He, Q.; Huo, D. A novel fluorescence probe for rapid and sensitive detection of tetracyclines residues based on silicon quantum dots. *Spectrochim. Acta A* **2020**, *240*, 118463. [[CrossRef](#)] [[PubMed](#)]
4. Wang, J.; Chu, L.; Wojnarovits, L.; Takacs, E. Occurrence and fate of antibiotics, antibiotic resistant genes (ARGs) and antibiotic resistant bacteria (ARB) in municipal wastewater treatment plant: An overview. *Sci. Total Environ.* **2020**, *744*, 140997. [[CrossRef](#)] [[PubMed](#)]
5. Kovalakova, P.; Cizmas, L.; McDonald, T.J.; Marsalek, B.; Feng, M.; Sharma, V.K. Occurrence and toxicity of antibiotics in the aquatic environment: A review. *Chemosphere* **2020**, *251*, 126351. [[CrossRef](#)]
6. Oliver, J.P.; Gooch, C.A.; Lansing, S.; Schueler, J.; Hurst, J.J.; Sassoubre, L.; Crossette, E.M.; Aga, D.S. Invited review: Fate of antibiotic residues, antibiotic-resistant bacteria, and antibiotic resistance genes in US dairy manure management systems. *J. Dairy Sci.* **2020**, *103*, 1051–1071. [[CrossRef](#)]
7. Zainab, S.M.; Junaid, M.; Xu, N.; Malik, R.N. Antibiotics and antibiotic resistant genes (ARGs) in groundwater: A global review on dissemination, sources, interactions, environmental and human health risks. *Water Res.* **2020**, *187*, 116455. [[CrossRef](#)]
8. Wu, Q.; Shabbir, M.A.B.; Peng, D.; Yuan, Z.; Wang, Y. Microbiological inhibition-based method for screening and identifying of antibiotic residues in milk, chicken egg and honey. *Food Chem.* **2021**, *363*, 130074. [[CrossRef](#)]
9. Pham, T.N.M.; Le, T.B.; Le, D.D.; Ha, T.H.; Nguyen, N.S.; Pham, T.D.; Hauser, P.C.; Nguyen, T.A.H.; Mai, T.D. Determination of carbapenem antibiotics using a purpose-made capillary electrophoresis instrument with contactless conductivity detection. *J. Pharm. Biomed.* **2020**, *178*, 112906. [[CrossRef](#)]

10. Ravikumar, A.; Panneerselvam, P. A novel fluorescent sensing platform based on metal-polydopamine frameworks for the dual detection of kanamycin and oxytetracycline. *Analyst* **2019**, *144*, 2337–2344. [[CrossRef](#)]
11. Zhou, X.; Wang, L.; Shen, G.; Zhang, D.; Xie, J.; Mamut, A.; Huang, W.; Zhou, S. Colorimetric determination of ofloxacin using unmodified aptamers and the aggregation of gold nanoparticles. *Microchim. Acta* **2018**, *185*, 355. [[CrossRef](#)] [[PubMed](#)]
12. Fang, X.; Chen, X.; Liu, Y.; Li, Q.; Zeng, Z.; Maiyalagan, T.; Mao, S. Nanocomposites of Zr(IV)-based metal-organic frameworks and reduced graphene oxide for electrochemically sensing ciprofloxacin in water. *Acs Appl. Nano Mater.* **2019**, *2*, 2367–2376. [[CrossRef](#)]
13. Acaroz, U.; Dietrich, R.; Knauer, M.; Märtlbauer, E. Development of a generic enzyme-immunoassay for the detection of fluoro(quinolone)-residues in foodstuffs based on a highly sensitive monoclonal antibody. *Food Anal. Method.* **2019**, *13*, 780–792. [[CrossRef](#)]
14. Soheili, V.; Taghdisi, S.M.; Hassanzadeh Khayat, M.; Fazly Bazzaz, B.S.; Ramezani, M.; Abnous, K. Colorimetric and ratiometric aggregation assay for streptomycin using gold nanoparticles and a new and highly specific aptamer. *Microchim. Acta* **2016**, *183*, 1687–1697. [[CrossRef](#)]
15. Wang, G.; Zhang, H.C.; Liu, J.; Wang, J.P. A receptor-based chemiluminescence enzyme linked immunosorbent assay for determination of tetracyclines in milk. *Anal. Biochem.* **2019**, *564–565*, 40–46. [[CrossRef](#)] [[PubMed](#)]
16. Jiang, H.; Lin, H.; Lin, J.; Yao-Say Solomon Adade, S.; Chen, Q.; Xue, Z.; Chan, C. Non-destructive detection of multi-component heavy metals in corn oil using nano-modified colorimetric sensor combined with near-infrared spectroscopy. *Food Control* **2022**, *133*, 108640. [[CrossRef](#)]
17. Yu, Y.; Naik, S.S.; Oh, Y.; Theerthagiri, J.; Lee, S.J.; Choi, M.Y. Lignin-mediated green synthesis of functionalized gold nanoparticles via pulsed laser technique for selective colorimetric detection of lead ions in aqueous media. *J. Hazard. Mater.* **2021**, *420*, 126585. [[CrossRef](#)]
18. Unnikrishnan, B.; Lien, C.W.; Chu, H.W.; Huang, C.C. A review on metal nanozyme-based sensing of heavy metal ions: Challenges and future perspectives. *J. Hazard. Mater.* **2021**, *401*, 123397. [[CrossRef](#)]
19. Zhong, Y.H.; He, Y.; Zhou, H.Q.; Zheng, S.L.; Zeng, Q.; Chung, L.H.; Liao, W.M.; He, J. Enhanced stability and colorimetric detection on Ag(I) ions of a methylthio-functionalized Zn(II) metal-organic framework. *J. Mater. Chem. C* **2021**, *9*, 5088–5092. [[CrossRef](#)]
20. Chen, Z.; Qian, S.; Chen, J.; Cai, J.; Wu, S.; Cai, Z. Protein-templated gold nanoclusters based sensor for off-on detection of ciprofloxacin with a high selectivity. *Talanta* **2012**, *94*, 240–245. [[CrossRef](#)]
21. Nilghaz, A.; Lu, X. Detection of antibiotic residues in pork using paper-based microfluidic device coupled with filtration and concentration. *Anal. Chim. Acta* **2019**, *1046*, 163–169. [[CrossRef](#)] [[PubMed](#)]
22. Zhao, Q.; Yan, H.; Liu, P.; Yao, Y.; Wu, Y.; Zhang, J.; Li, H.; Gong, X.; Chang, J. An ultra-sensitive and colorimetric sensor for copper and iron based on glutathione-functionalized gold nanoclusters. *Anal. Chim. Acta* **2016**, *948*, 73–79. [[CrossRef](#)]
23. Ma, S.; Wang, J.; Yang, G.; Yang, J.; Ding, D.; Zhang, M. Copper(II) ions enhance the peroxidase-like activity and stability of keratin-capped gold nanoclusters for the colorimetric detection of glucose. *Microchim. Acta* **2019**, *186*, 271. [[CrossRef](#)] [[PubMed](#)]
24. Shi, Y.; Wang, J.; Mu, K.; Liu, S.; Yang, G.; Zhang, M.; Yang, J. Copper (II) ion-modified gold nanoclusters as peroxidase mimetics for the colorimetric detection of pyrophosphate. *Sensors* **2021**, *21*, 5538. [[CrossRef](#)]
25. Song, Y.; Qiao, J.; Liu, W.; Qi, L. Enhancement of gold nanoclusters-based peroxidase nanozymes for detection of tetracycline. *Microchem. J.* **2020**, *157*, 104871. [[CrossRef](#)]
26. Cowger, T.A.; Yang, Y.; Rink, D.E.; Todd, T.; Chen, H.; Shen, Y.; Yan, Y.; Xie, J. Protein-adsorbed magnetic-nanoparticle-mediated assay for rapid detection of bacterial antibiotic resistance. *Bioconjug. Chem.* **2017**, *28*, 890–896. [[CrossRef](#)] [[PubMed](#)]
27. Tomita, S.; Niwa, O.; Kurita, R. Artificial modification of an enzyme for construction of cross-reactive polyion complexes to fingerprint signatures of proteins and mammalian cells. *Anal. Chem.* **2016**, *88*, 9079–9086. [[CrossRef](#)]
28. Yan, P.; Li, X.; Dong, Y.; Li, B.; Wu, Y. A pH-based sensor array for the detection and identification of proteins using CdSe/ZnS quantum dots as an indicator. *Analyst* **2019**, *144*, 2891–2897. [[CrossRef](#)]
29. Mao, Y.; Cui, S.; Li, W.; Fan, X.; Liu, Y.; Xu, S.; Luo, X. A lab-on-a-carbon nanodot sensor array for simultaneous pattern recognition of multiple antibiotics. *Sensor. Actuat. B-Chem.* **2019**, *296*, 126694. [[CrossRef](#)]
30. Yan, P.; Ding, Z.; Li, X.; Dong, Y.; Fu, T.; Wu, Y. Colorimetric sensor array based on wulff-type boronate functionalized AgNPs at various pH for bacteria identification. *Anal. Chem.* **2019**, *91*, 12134–12137. [[CrossRef](#)]
31. Zhang, Z.; Zhu, N.; Zou, Y.; Wu, X.; Qu, G.; Shi, J. A novel, enzyme-linked immunosorbent assay based on the catalysis of AuNCs@BSA-induced signal amplification for the detection of dibutyl phthalate. *Talanta* **2018**, *179*, 64–69. [[CrossRef](#)]
32. Zhou, Y.; Ma, Z. Colorimetric detection of Hg<sup>2+</sup> by Au nanoparticles formed by H<sub>2</sub>O<sub>2</sub> reduction of HAuCl<sub>4</sub> using Au nanoclusters as the catalyst. *Sensor. Actuat. B-Chem.* **2017**, *241*, 1063–1068. [[CrossRef](#)]
33. Li, S.; Zhang, L.; Jiang, Y.; Zhu, S.; Lv, X.; Duan, Z.; Wang, H. In-site encapsulating gold “nanowires” into hemin-coupled protein scaffolds through biomimetic assembly towards the nanocomposites with strong catalysis, electrocatalysis, and fluorescence properties. *Nanoscale* **2017**, *9*, 16005–16011. [[CrossRef](#)] [[PubMed](#)]
34. Chen, Y.; Wang, A.; Zhang, Y.; Bao, R.; Tian, X.; Li, J. Electro-Fenton degradation of antibiotic ciprofloxacin (CIP): Formation of Fe<sup>3+</sup>-CIP chelate and its effect on catalytic behavior of Fe<sup>2+</sup>/Fe<sup>3+</sup> and CIP mineralization. *Electrochim. Acta* **2017**, *256*, 185–195. [[CrossRef](#)]

35. Puicharla, R.; Mohapatra, D.P.; Brar, S.K.; Drogui, P.; Auger, S.; Surampalli, R.Y. A persistent antibiotic partitioning and co-relation with metals in wastewater treatment plant-chlortetracycline. *J. Environ. Chem. Engl.* **2014**, *2*, 1596–1603. [[CrossRef](#)]
36. Yu, M.; Zhu, Z.; Wang, H.; Li, L.; Fu, F.; Song, Y.; Song, E. Antibiotics mediated facile one-pot synthesis of gold nanoclusters as fluorescent sensor for ferric ions. *Biosens. Bioelectron.* **2017**, *91*, 143–148. [[CrossRef](#)] [[PubMed](#)]
37. Jin, X.; Qiu, S.; Wu, K.; Jia, M.; Wang, F.; Gu, C.; Zhang, A.; Jiang, X. The effect of  $\text{Cu}^{2+}$  chelation on the direct photolysis of oxytetracycline: A study assisted by spectroscopy analysis and DFT calculation. *Environ. Pollut.* **2016**, *214*, 831–839. [[CrossRef](#)]
38. Wang, Y.W.; Tang, H.; Wu, D.; Liu, D.; Liu, Y.; Cao, A.; Wang, H. Enhanced bactericidal toxicity of silver nanoparticles by the antibiotic gentamicin. *Environ. Sci. Nano* **2016**, *3*, 788–798. [[CrossRef](#)]
39. Wei, X.; Chen, J.; Xie, Q.; Zhang, S.; Li, Y.; Zhang, Y.; Xie, H. Photochemical behavior of antibiotics impacted by complexation effects of concomitant metals: A case for ciprofloxacin and Cu(II). *Environ. Sci. Proc. Imp.* **2015**, *17*, 1220–1227. [[CrossRef](#)]
40. Pereira, J.H.O.S.; Queirós, D.B.; Reis, A.C.; Nunes, O.C.; Borges, M.T.; Boaventura, R.A.R.; Vilar, V.J.P. Process enhancement at near neutral pH of a homogeneous photo-fenton reaction using ferric-carboxylate complexes: Application to oxytetracycline degradation. *Chem. Eng. J.* **2014**, *253*, 217–228. [[CrossRef](#)]
41. Wang, H.; Yao, H.; Sun, P.; Li, D.; Huang, C.H. Transformation of tetracycline antibiotics and Fe(II) and Fe(III) species induced by their complexation. *Environ. Sci. Technol.* **2016**, *50*, 145–153. [[CrossRef](#)] [[PubMed](#)]
42. Liu, D.; Pan, X.; Mu, W.; Li, C.; Han, X. Detection of tetracycline in water using glutathione-protected fluorescent gold nanoclusters. *Anal. Sci.* **2019**, *35*, 367–370. [[CrossRef](#)] [[PubMed](#)]
43. Fu, B.; Zheng, X.; Li, H.; Ding, L.; Wang, F.; Guo, D.-Y.; Yang, W.; Pan, Q. A highly stable, rapid and sensitive fluorescent probe for ciprofloxacin based on  $\text{Al}^{3+}$ -enhanced fluorescence of gold nanoclusters. *Sensor. Actuat. B-Chem.* **2021**, *346*, 130502. [[CrossRef](#)]
44. Wei, W.; He, J.; Wang, Y.; Kong, M. Ratiometric method based on silicon nanodots and  $\text{Eu}^{3+}$  system for highly-sensitive detection of tetracyclines. *Talanta* **2019**, *204*, 491–498. [[CrossRef](#)]